J Therm Anal Calorim (2017) 128:957–969
DOI 10.1007/s10973-016-6018-1

Synthesis, spectral, thermal and insulin-enhancing properties of oxovanadium(IV) complexes of metformin Schiff-bases

Marwa A. Mahmoud[1] · Sawsan A. Zaitone[2] · Alaa M. Ammar[3] · Shehab A. Sallam[3]

Received: 14 July 2016 / Accepted: 26 November 2016 / Published online: 8 December 2016

Abstract A series of VO^{2+} complexes of Schiff-bases of metformin with each of salicylaldehyde (HL^1); 2,3-dihydroxybenzaldehyde (H_2L^2); 2,4-dihydroxybenzaldehyde (H_2L^3); 2,5-dihydroxybenzaldehyde (H_2L^4); 3,4-dihydroxybenzaldehyde (H_2L^5); and 2-hydroxynaphthaldehyde (HL^6) were synthesized by template reaction. The new compounds are characterized through elemental analysis, conductivity measurements, magnetic moment, IR, UV–Vis, ESR and mass spectroscopy. The complexes have square pyramidal structure with μ values of pentacoordinated vanadyl ion. TG, DTG and DTA confirm the proposed stereochemistry, and a mechanism of thermal decomposition was suggested. Mice treated with the complexes $[VOL^1H_2O]\cdot 1½H_2O$ and $[VOHL^4H_2O]\cdot 2H_2O$ showed glucose-lowering effect of 59.31, 58.79% (20 mg kg^{-1}) and 64.98, 74.8% (40 mg kg^{-1}) compared to metformin.

Keywords Metformin Schiff-bases · VO^{2+} complexes · Spectral and thermal properties · Antidiabetes mellitus

✉ Shehab A. Sallam
shehabsallam@yahoo.com

[1] Department of Science and Mathematics Engineering, Faculty of Petroleum and Mining Engineering, Suez University, Suez, Egypt

[2] Department of Pharmacology and Toxicology, Faculty of Pharmacy, Suez Canal University, Ismailia, Egypt

[3] Department of Chemistry, Faculty of Science, Suez Canal University, Ismailia, Egypt

Introduction

Vanadium complexes were found to present antimicrobial, antitumor and insulin-enhancing effects [1]. Oxovanadium(IV) sulfate has been demonstrated to possess oral insulin-like activity similar to that of the vanadates, with lowered toxicity [2]. Neutral oxovanadium(IV) complexes, with a variety of coordination environments, have been examined as potential insulin-enhancing agents ranging from the common $VO(O_4)$ to $VO(N_2O_2)$, $VO(N_4)$, $VO(S_4)$, $VO(S_2O_2)$ and $VO(N_2S_2)$ [3–6].

Blood glucose levels of rats with alloxan-induced diabetes have dropped from hyperglycemic levels to hypoglycemic ones after treatment with bis-salicylidine ethylenediaminato oxovanadium(IV) complex [7]. In vivo insulin-mimetic activity of [*N*,*N*′-1,3-propyl-bis(salicyladimine)]oxovanadium(IV) has been tested [8]. Oxovanadium(IV) and (V) complexes of acetylpyridine-derived semicarbazones were able to enhance glucose uptake and to inhibit glycerol release from adipocytes which indicate their potential to act as insulin mimics [9]. Complexes of $VOCl_2$ with 2-pyridineformamide thiosemicarbazones inhibited glycerol release in a similar way to that observed with insulin but showed a low enhancing effect on glucose uptake by rat adipocytes [10]. A series of oxovanadium(IV) symmetrical tetradentate Schiff-base complexes have been isolated from the reaction of $VOSO_4$ with Schiff-bases obtained from the condensation of 2-hydroxybenzophenone or 2-hydroxy-5-chlorosalicylaldehyde with various aliphatic diamines [11]. Recently, new insulin-mimetic and hypoglycemic heterobinuclear zinc(II)/oxovanadium(IV) complex was synthesized and characterized [12].

Metformin hydrochloride (MF·HCl) (1,1-dimethylbiguanide) is an oral hypoglycemic agent which is

commonly prescribed for the treatment of DM II [13]. There is much interest in MF ligand and its transition metal complexes which are cationic in nature [14–19]. Also, it was shown that vanadyl–biguanide complexes are potential synergistic insulin mimics [20]. Regarding the potential functions of Schiff-bases, Gao [21] has studied the antimicrobial activity of copper(II) complex derived from the condensation of MF with 2-pyridinecarbaldehyde. In addition, Ni(II) complexes with ligands that resulted in condensation of MF and pentane-2,4-dione were synthesized and characterized [22]. Thermal behavior of the complexes was also evaluated [17–19, 22]. Recently, new decavanates using metformin as counterion with formula $(H_2Metf)_3[V_{10}O_{28}]\cdot 8H_2O$ was shown to have pharmacological potential as a hypoglycemic, lipid-lowering and metabolic reagent [23].

In order to modulate the biological activity of MF and to correlate this activity with structure, a series of vanadium complexes with Schiff-bases of MF with salicylaldehyde (HL^1); 2,3-dihydroxybenzaldehyde (H_2L^2); 2,4-dihydroxybenzaldehyde (H_2L^3); 2,5-dihydroxybenzaldehyde (H_2L^4); 3,4-dihydroxybenzaldehyde (H_2L^5); and 2-hydroxynaphthaldehyde (HL^6) were synthesized by template reaction. The resulting complexes were characterized using elemental analysis, conductivity measurements, magnetic moment values, spectral analysis (UV–Vis, IR, ESR, MS), and TG, DTG and DTA. Insulin-like activity of the complexes was evaluated in alloxan-induced Swiss albino mice.

Experimental

Materials

All chemicals used in this study are of A.R. or equivalent grade and were used without further purification. Salicylaldehyde; 2-hydroxynaphthaldehyde; 2,3-dihydroxybenzaldehyde; 2,4-dihydroxybenzaldehyde; 2,5-dihydroxybenzaldehyde; and 3,4-dihydroxybenzaldehyde (Koch-Light Laboratories) were used as such. Metformin HCl was purchased from El-Nasr Company for Pharmaceutical Chemicals, Cairo, Egypt. $VOSO_4\cdot H_2O$ was obtained from Aldrich Chemical Company. Alloxan monohydrate powder was purchased from Sigma-Aldrich, St. Louis, MO, USA.

Synthesis of the Schiff-bases

The Schiff-bases have been prepared by addition of methanolic MF solution to a methanolic solution of the aldehyde in 1:1 ratio in basic medium [24]. The mixture was refluxed with continuous stirring over water bath for two hours. The solution turned to yellow color indicating the formation of the Schiff-base. Only, HL^1 Schiff-base was isolated in the solid state, dried under vacuum and recrystallized from methanol (m.p. 195 °C). The purity was checked by TLC using methanol–chloroform solvent mixture (1:10 v/v). HL^1 Schiff-base was characterized using C, H and N analyses, ^{1}H NMR, UV–Vis and GC-mass spectra as well as TG, DTG and DTA. Its structure is shown in Structure 1.

Template synthesis of the complexes

All complexes were prepared according to the following procedure. Solution of $VOSO_4\cdot H_2O$ (1 mmol, 0.18 g) in 5 mL of distilled water was added dropwise to methanolic solution of the Schiff-base (1 mmol) prepared in the previous step. The mixture was refluxed on water bath for 2 h with stirring during which a deep green solution is formed (pH = 4–4.5), after which NH_4OH is added dropwise till the complex is precipitated (pH = 6–7). Stirring is continued for another 1 h at room temperature, and the complex is filtered, washed thoroughly with water and hot methanol and dried under vacuum. The following series of complexes were obtained: $[VOL^1H_2O]\cdot 1\frac{1}{2}H_2O$ **(1)**, $[VOHL^2H_2O]\cdot 2H_2O$ **(2)**, $[VOHL^3H_2O]\cdot 2H_2O$ **(3)**, $[VOHL^4H_2O]\cdot 2H_2O$ **(4)**, $[VOL^5(H_2O)_2]\cdot 2H_2O\cdot$**(5)**, $[VOL^6H_2O]\cdot 2H_2O$ **(6)**.

Physical measurements

C, H and N were estimated using a Heraeus CHN Rapid Analyzer. The IR spectra were recorded (KBr disk) in the 400–4000 cm^{-1} range on Bruker Vector-22 spectrometer. Mass spectral data analyses of the complexes were carried out on Varian MAT-711 spectrometer. The electronic absorption spectra were obtained using 10^{-3} M DMSO solution in 1-cm quartz cell using UV-1601PC Shimadzu spectrophotometer. Magnetic susceptibility measurements were taken using the modified Gouy method [25] on MSB-MK1 balance at room temperature. Solid-state X-band ESR spectra were recorded at 298 K on a Bruker EMX spectrometer. TG, DTG and DTA were performed on Shimadzu H-60 thermal analyzer under a dynamic flow of nitrogen (30 mL min^{-1}) and heating rate 10 °C min^{-1} from ambient temperature to 750 °C. Electrical conductivity measurements were taken at room temperature on freshly

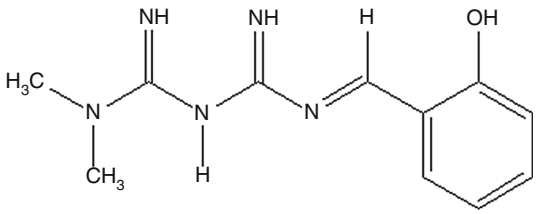

Structure 1 HL^1 Schiff-base

prepared 10^{-3} M DMSO solutions using WTW conductivity meter fitted with L100 conductivity cell. Metal content was obtained by EDTA titration using PAN indicator and acetate buffer.

Experimental assay

Experimental protocols were approved by the Research Ethics Committee (License Number 201410A4) at the Faculty of Pharmacy, Suez Canal University, Ismailia, Egypt. Animal suffering during handling or injection was kept at minimal. Healthy male Swiss albino mice with original body weight 18–30 g were used in the current experiment. Mice were provided by the National Authority of Vaccines (Cairo, Egypt) and were maintained under suitable laboratory conditions with a normal light–dark cycle. They were housed in a clean polyethylene cages with food and water ad libitum and were allowed to acclimatize for ten days before starting the experiment.

Preparation of drugs and induction of diabetes mellitus in experimental animals

Alloxan monohydrated was freshly prepared just before use by dissolution in saline. Metformin and the test complexes were dissolved in DMSO/saline 1:5 (v/v).

Mice were fasted overnight and injected with alloxan (150 mg kg^{-1} day^{-1}, i.p., daily schedule) [26] in order to induce experimental diabetes mellitus. One week after alloxan injection, hyperglycemia was confirmed by estimation of the level of fasting blood glucose using a blood sample from the tail vein employing a glucometer (BioSTC, USA). Mice with final blood glucose levels >200 mg dL^{-1} were considered diabetic and included in the experiment.

Experimental design

Diabetic mice were subjected to a therapeutic period (14 doses) of treatment with tested complexes and the standard metformin (20 or 40 mg kg^{-1}, i.p.). Mice were randomly allocated into different groups (six mice each) as follows:

1. vehicle (saline)
2. diabetic group
3. diabetic + metformin
4. diabetic + complex **1**
5. diabetic + complex **4**

Diabetic control mice received 14 doses of DMSO/saline solution (12 mL kg^{-1}, i.p.) at the same schedule reported for metformin and the test complexes.

At the end of the experiment, the percent of surviving mice in each group was recorded and groups with survival percent >50% were included in the following procedures.

Collection of blood samples

After the last day of drug treatment, mice were anesthetized with ether and killed by cervical dislocation. Blood samples were collected by cardiac puncture and centrifuged after standing for 30 min ($3000\times g$, 15 min) at room temperature. Sera were separated and stored at −20 °C until use for assay of total cholesterol as well as activities of ALT and AST.

Histopathological examination of pancreas

For dissection of the pancreas, a laparotomy was performed and the pancreas was immediately isolated and fixed overnight in 4% paraformaldehyde solution. Cross sections of 4 μm were cut and processed for routine staining with hematoxylin and eosin (H&E) and were used for histopathological examination under a light microscope (OPTICA). Photographs were then captured, and diameters of ten random islets of Langerhans in each section were determined using GIMP 2.8.14 software. Diameters were then averaged for each animal and compared to determine the effect of drugs on the diseased islets.

Statistical analyses

Data were collected, tabulated and expressed as the mean ± SEM and were analyzed using one-way analysis of variance (ANOVA) followed by Bonferroni's post hoc test, and significance was set at $P < 0.05$. Statistical analysis was performed using the SPSS program (SPSS Inc., Chicago, IL, USA).

Results and discussion

Vanadyl complexes of the metformin Schiff-bases

All the complexes are air-stable and remarkably soluble in DMSO and DMF, slightly soluble in MeOH and insoluble in benzene, acetone and diethyl ether. The complexes of VO^{2+} melt in the 200–178 °C range except the complex **1** which decomposes without melting above 390 °C. Elemental analysis show 1:1 (metal:ligand) stoichiometry for all the complexes. The analytical data and some physical properties of the complexes are shown in Table 1. The molar conductance values of 10^{-3} M DMSO solutions of the complexes are consistent with their non-electrolytic nature [27].

Infrared Spectra

The assignments of the IR bands of the vanadyl complexes have been made by comparing with the bands of HL^1 ligand

Table 1 Analytical data, conductivity and magnetic moments of the vanadyl complexes of the metformin Schiff-bases

Complex number	Color	Mol wt	Melting and dec. point/°C	Yield/%	Elemental analysis Found calcd./%				*Ω
					C	H	N	M	
1	Black green	342.21	>300	69	38.2	5.2	20.4	14.5	0.2
					38.4	5.2	20.3	14.8	
2	Black green	368.21	198	66	35.9	5.4	19.1	13.9	0.3
					35.8	5.1	19.0	13.8	
3	Olive green	368.21	190	58	35.5	5.6	19.1	13.7	0.3
					35.8	5.1	19.0	13.8	
4	Olive green	368.21	178	68	35.6	5.5	19.1	13.5	0.3
					35.8	5.1	19.0	13.8	
5	Black green	386.21	188	66	34.2	5.6	18.2	13.7	0.3
					34.1	5.4	18.1	13.1	
6	Deep green	402.21	200	68	44.8	5.1	17.5	12.5	0.4
					44.7	5.2	17.4	12.6	

* 10^{-3} M in DMSO, ohm^{-1} cm^2 mol^{-1}

and structurally similar molecules (Table 2). The major IR spectral features of the presented complexes indicate some characteristic bands of biguanide and Schiff-base moiety. The strong broad band ascribed to υ(OH) of the Schiff-base at 3456 cm^{-1} disappeared in the spectra of all vanadyl complexes which accounts for the deprotonation and coordination of the OH group [24]. The hydrated complexes have OH stretching frequencies as a broad band in the 3416–3389 cm^{-1} region. IR spectra of the complexes **1–4** and **6** show broad intense band in the 3291–3208 and 3128–3104 cm^{-1} range assignable to the stretching vibration of the N–H group. These bands were observed in the spectra of some complexes with biguanide Schiff-bases [21, 22]. The strong bands observed in the 1694–1673 and 1655–1650 cm^{-1} range can be attributed to υ(C=N) [28]. High values for stretching frequency of the azomethine group were observed with transition and non-transition metal complexes of MF ligand [19]. A band appearing in the 1571–1556 and 1276–1275 cm^{-1} interval has been assigned to symmetric and asymmetric N–C–N stretching [19]. The

Table 2 IR spectral data of the vanadyl complexes of the metformin Schiff-bases

Complex number	υ(H_2O) υ(OH)	υ(NH)	υ(C=N)	υ(N–C-N)	υ(C-O)	υ(V=O)	υ(M–O) υ(M–N)
HL^1 [24]	3456 m	3370 s	1643 s	1498 m	1291 m		
		3297 s	1599 s		1230 m	–	–
		3172 s	1564 s				
1	3414 s	3208 m	1673 s	1571 m	1276 m	978 s	595 s
		3104 m	1655 s		1236 m		520 m
2	3410 s	3256 m	1680 s	1556 m	1275 m	978 s	594 s
		3127 m	1651 s		1229 m		480 m
3	3393 s	3291 m	1686 s	1566 m	1275 m	990 s	593 s
		3126 m	1651 s		1238 m		480 m
4	3393 s	3270 m	1684 s	1565 m	1276 m	983 s	596 s
		3128 m	1652 s		1239 m		482 m
5	3416 s	3387 m	1642 s	1510 m	1286 m	982 s	597 m
		3282 m	1594 s				–
		3160 m					
6	3389 s	3287 m	1694 s	1568 m	1275 m	976 s	593 s
		3106 m	1650 s		1241 m		479 m

s strong, *m* medium

band assignable to υ(C–O) is recorded as a medium frequency in the 1241–1229 cm^{-1} region confirming deprotonation and coordination of the phenolic oxygen to the VO^{2+} ion [29]. Characteristic stretching frequencies of the V=O bond in oxovanadium(IV) complexes generally occur in the region 930–1030 cm^{-1} [30]. In the present work, all vanadium complexes exhibit a strong band in the range 990–976 cm^{-1} which have assigned to υ(V=O) in a monomeric square pyramidal geometry [11, 31]. The nature of metal–ligand bonding is confirmed by the newly formed bands at 596–593 and 520–479 cm^{-1} in the spectra of the complexes which are tentatively assigned to ν(V–O) and ν(V–N), respectively [32].

The complex **5** has IR data showing υ(NH), υ(C=N) and υ(N–C–N) at 3387, 3282, 3160; 1642, 1594 and 1510 cm^{-1}. These values are different from the rest of the complexes and nearly similar in number and position to the free HL^1 Schiff-base frequencies. This indicates the non-participation of either the azomethine or C=NH groups in bonding in the complex. Also, in this complex, υ(C–O) appears as medium band at 1286 cm^{-1}, while the other complexes show this band at lower frequency. The V–N frequency is not present in the IR spectrum of the complex and only V–O appears at 597 cm^{-1}. Also, VO^{2+} is a hard acid, so it is expected to prefer bonding through the two oxygen atoms of the hydroxyl groups of the Schiff-base after deprotonation forming five-membered ring which may be more stable than forming six-membered ring through the nitrogen atoms [33].

Magnetic and UV–Vis spectra

All the prepared complexes are paramagnetic in the solid state with the electronic configuration $[Ar]3d^1$. Vanadium(IV) has one unpaired electron with spin-only formula predicting a magnetic moment of 1.73 B.M. The experimental values are in the range 1.79–1.72 B.M. for the vanadyl complexes (Table 3). These values are in the range recorded for some monomeric pentacoordinated vanadyl Schiff-bases complexes [8–11] and are consistent with square pyramidal geometry around the central metal ion [34].

Electronic absorption spectral data of the oxovanadium(IV) complexes in DMSO solutions along with their assignments are given in Table 3. The transitions that attributed to $\pi \rightarrow \pi^*$ and $n \rightarrow \pi^*$ in the 316–257 and 365–312 nm region in the UV spectra of the complexes are blueshifted compared to HL^1 spectrum, indicating coordination of the imine nitrogen to the vanadyl ion [19].

Generally, vanadyl complexes have molecular orbital scheme (based on $VOSO_4.5H_2O$ spectrum, C_{4v} symmetry) which give rise to three d–d bands [35]. They are assigned as $xy \rightarrow xz$, yz (band I), $xy \rightarrow x^2 - y^2$ (band II) and $xy \rightarrow z^2$ (band III) in order of decreasing energy [36]. The spectra of the complexes **5** and **6** show the $xy \rightarrow x^2 - y^2$ transition at 519 and 572 nm, while the complex **3** shows the $xy \rightarrow z^2$ transition at 425 nm. All the complexes under study indicate the $xy \rightarrow xz$, yz transition in the 890–870 nm region. The electronic spectra are typical of five-coordinated vanadyl complexes which were previously observed with other vanadyl Schiff-base complexes [11, 37–39].

Mass spectra

The mass spectra of the complexes **3** and **5** were analyzed to determine their molecular weight and fragmentation pattern. They give mononuclear species in the positive ion spectra under MS conditions employed. The parent ion is observed for the complex **5**, while it is not for the first one as the lattice water is readily lost. The complexes continue losing the coordinated water followed by $HN(CH_3)_2$ species and ending with rest of the Schiff-bases. The obtained results are given in Table 4.

ESR spectra

ESR spectra of all the oxovanadium(IV) complexes were recorded in polycrystalline state at room temperature, and the spectral parameters are summarized in Table 5. The ESR spectrum of the complex **2** displayed well-resolved axial anisotropy (Fig. 1) with $g_{\parallel} = 1.95$ and $g_{\perp} = 1.99$. The spectrum shows two sets of eight-line pattern, characteristic of an unpaired electron being coupled to the vanadium nuclear spin ($I = 7/2$). The anisotropic hyperfine parameters were calculated ($A_{\parallel} = 180$ and $A_{\perp} = 66$ cm^{-1}). The complexes **3**, **4** and **5** in polycrystalline state at room temperature are axial with $g_{\parallel} = 1.968$, 1.977 and 1.96 and $g_{\perp} = 1.986$, 1.985 and 1.988 and anisotropic hyperfine parameters $A_{\parallel} = 178$, 177.9 and 173×10^{-4} cm^{-1} and $A_{\perp} = 67.9$, 68.8 and 63.2×10^{-4} cm^{-1}. The isotropic EPR parameters g_{iso} and A_{iso} can be determined from the anisotropic parameters, using the relations $g_{iso} = 1/3(2\ g_{\perp} + g_{\parallel})$ and $A_{iso} = 1/3(2\ A_{\perp} + A_{\parallel})$. The measured value of $g_{\parallel}$, $g_{\perp}$, $A_{\parallel}$ and $A_{\perp}$ are in a good agreement for a square pyramidal structure [40] and are reported in Table 5. The g values are generally lower than the free electron value, $g_e = 2.002$. This lowering can be related to the spin–orbit interaction of the ground state, d_{xy} level, with the low-lying excited states [41]. ESR spectra of the complexes **1** and **6** exhibit isotropic spectra with g_{iso} values of 1.983 and 1.982.

Structure of the complexes

According to the above-mentioned data, the ligands $HL^{1,6}$ and H_2L^{2-4} behave as a dibasic tridentate ligands where the vanadyl ion has a square pyramidal structure with the

Table 3 Electronic spectra and magnetic moments of the vanadyl complexes of the metformin Schiff-bases

Complex number	Band/nm	Assignment	Proposed structure	*μ_{eff} B.M.
1	258, 261	$\pi \rightarrow \pi^*$	†Spy	1.72
	324	$n \rightarrow \pi^*$		
	870	$xy \rightarrow xz, yz$ (band I)		
2	257, 281	$\pi \rightarrow \pi^*$	Spy	1.74
	314	$n \rightarrow \pi^*$		
	889	$xy \rightarrow xz, yz$ (band I)		
3	257, 286	$\pi \rightarrow \pi^*$	Spy	1.79
	323	$n \rightarrow \pi^*$		
	425	$xy \rightarrow z^2$ (band III)		
	847	$xy \rightarrow xz, yz$ (band I)		
4	263	$\pi \rightarrow \pi^*$	Spy	1.72
	312	$n \rightarrow \pi^*$		
	890	$xy \rightarrow xz, yz$ (band I)		
5	259, 268	$\pi \rightarrow \pi^*$	Spy	1.75
	320	$n \rightarrow \pi^*$		
	519	$xy \rightarrow x^2 - y^2$ (band II)		
	858	$xy \rightarrow xz, yz$ (band I)		
6	316	$\pi \rightarrow \pi^*$	Spy	1.77
	365	$n \rightarrow \pi^*$		
	572	$xy \rightarrow x^2 - y^2$ (band II)		
	885	$xy \rightarrow xz, yz$ (band I)		

† Spy = square pyramid

* $T = 298$ °K

Table 4 Mass fragmentation pattern of the complexes **3** and **5**

Complex number	*m/z*		Rel. Int.	Wt. loss	Lost species	Assignment
	Calcd.	Found				
3	368.21	–	–	–	–	$[VOHL^3H_2O]\cdot 2H_2O$
	332.94	331.2	54	36	$2H_2O$	$[VOL^3H_2O]^{-1}$
	314.94	314.2	20	18	H_2O	$[VOL^3]$
	269.24	269.2	54	45	$HN(CH_3)_2$	$[VO(0.8L^3)]$
	82.94	83.1	4	186	$0.8L^3$	$[VO_2]$
	66.94	63.4	10	8	$½O_2$	[VO]
5	386.21	386.1	79	–	–	$[VOL^5(H_2O)_2]\cdot 2H_2O$
	368.21	368.1	10	18	H_2O	$[VOL^5(H_2O)_2]\cdot H_2O$
	332.21	333.1	98	36	$2H_2O$	$[VOL^5H_2O]^{+1}$
	287.21	288.1	68	45	$HN(CH_3)_2$	$[VO(0.8L^5)H_2O]^{+1}$
	269.21	270.1	57	18	H_2O	$[VO(0.8L^5)]^{+1}$
	82.94	83.05	5	202	$0.8L^5$	$[VO_2]$
	66.94	63.5	64	8	$½O_2$	[VO]

oxo-ligand in the axial position. In the equatorial plane, VO^{2+} is coordinated to the Schiff-bases through the azomethine nitrogen, phenolic oxygen after deprotonation and the ionized C=NH group of the metformin (Structure 2). This ionization process was observed and discussed with other complexes of MF with transition metals

Table 5 ESR parameters of the vanadyl complexes of the metformin Schiff-bases

Complex number	ESR parameters (298 °K)					
	$g_{\parallel}$	$g_{\perp}$	$g_{iso/av}$	$A_{\parallel}$	$A_{\perp}10^{-4}$ cm	$A_{iso/av}$
2	1.95	1.99	1.976	180	66	104
3	1.968	1.986	1.98	178	68	103
4	1.977	1.985	1.982	177	69	105
5	1.96	1.988	1.978	173	63	100

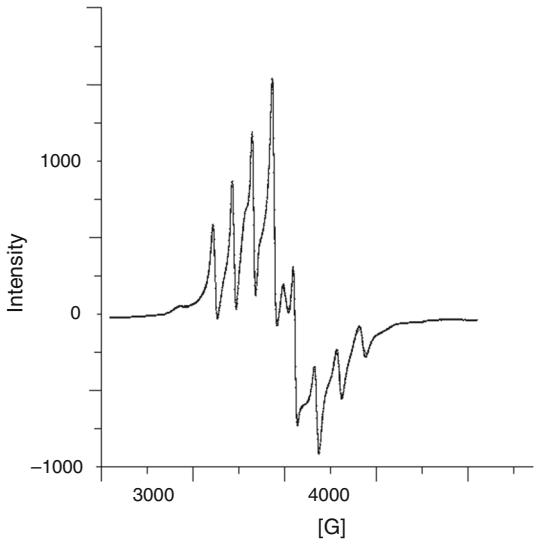

Fig. 1 Solid-state ESR spectrum of the complex (**2**)

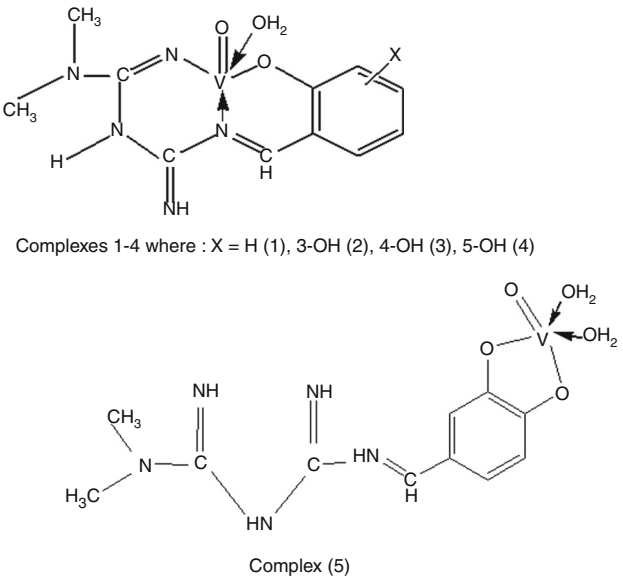

Structure 2 Complexes **1–5**

[14, 16, 20, 42, 43]. H_2L^5 behave as dibasic bidentate ligand by deprotonation of the phenolic hydroxyl groups, and the VO^{2+} forms covalent bond with the oxygen ions in O_4 chromophore in the equatorial plane using two H_2O molecules.

Thermal analysis

Thermal behavior of the analytically characterized vanadyl complexes of the metformin Schiff-bases has been studied through TG, DTG and DTA (Fig. 2 is an example). The phenomenological aspects are given in Tables 6 and 7.

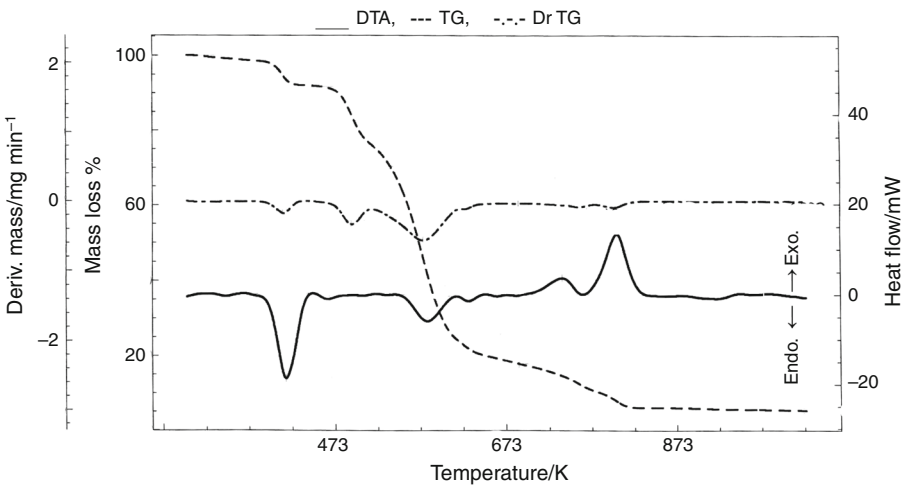

Fig. 2 TG, DTG and DTA of the complex (**2**)

Table 6 TG and DTG of the vanadyl complexes of the metformin Schiff-bases

Complex number	Temp. range/°C	DTG/ °C	Mass loss %		Process	Expected product/s	Residue % and type Found (Calcd.) %
			Found	Calcd.			
HL[1] [24]	160–293	258	19.17	19.29	Partial decomposition	$HN(CH_3)_2$	20.1
	294–422	351	30.14	30.44	Ligand decomposition	$HN(C{=}NH)_2$	(19.29)
	423–600	503	30.25	30.32	Final decomposition	0.13L	Carbonaceous material
1	58–125	66	7.91	7.86	Dehydration	$1½H_2O$	VO
	126–200	152	12.45	13.11	Partial decomposition	$NH(CH_3)_2$	20.87
	201–378	364	5.28	5.24	Coordinated water	H_2O	(19.50)
	379–522	415	52.85	53.91	Ligand decomposition	0.8L	
		467					
2	62–173	139	9.68	9.77	Dehydration	$2H_2O$	V
	174–272	218	12.89	12.22	Partial decomposition	$NH(CH_3)_2$	13.88
	273–343	302	5.25	4.89	Coordinated water	H_2O	(13.83)
	343–371	352	53.89	54.39	Ligand decomposition	0.8L	
	482–565	527	4.17	4.34	Reduction	$½O_2$	
3	50–175	141	9.65	9.77	Dehydration	$2H_2O$	V
	176–258	219	12.83	12.22	Partial decomposition	$NH(CH_3)_2$	13.50
	259–348	303	5.21	4.89	Coordinated water	H_2O	(13.83)
	348–375	352	53.89	54.39	Ligand decomposition	0.8L	
	496–543	523	4.50	4.34	Reduction	$½O_2$	
4	56–193	138	9.69	9.77	Dehydration	$2H_2O$	V
	194–256	216	12.10	12.22	Partial decomposition	$NH(CH_3)_2$	13.44
	257–344	307	5.18	4.89	Coordinated water	H_2O	(13.83)
	244–372	356	54.89	54.39	Ligand decomposition	0.8L	
	449–551	507	4.42	4.34	Reduction	$½O_2$	
5	41–115	68	4.17	4.66	Dehydration	H_2O	V
	116–174	133	4.23	4.66	Dehydration	H_2O	12.86
	175–274	225	15.77	16.31	Partial decomposition + Coordinated water	$HN(CH_3)_2$ H_2O	(13.19)
	275–374	318	22.95	23.04	Coordinated water + Ligand decomposition	H_2O $HN(CH{=}NH)_2$	
	375–530	477	32.27	32.36	Final decomposition	$C_6H_6 + H_2O + HN{=}CH$	
	531–559	539	6.10	6.21	Reduction	$¾O_2$	
6	44–163	137	8.33	8.95	Dehydration	$2H_2O$	V
	164–243	205	11.19	11.16	Partial decomposition	$HN(CH_3)_2$	12.51
	243–333	278	4.48	4.41	Coordinated water	H_2O	(12.66)
	334–472	375	58.61	58.74	Ligand decomposition	0.84L	
		441			Final decomposition		
	472–567	516	4.17	3.97	Reduction	$½O_2$	

The first decomposition step involves dehydration which takes place at 66, 139, 141, 138 and 137 °C for the complexes **1–4** and **6**. Mass losses recorded during this step are (found/calc.): 7.91/7.86%, 9.69–9.65/9.77% and 8.33/8.95% associated with endothermic DTA peaks at 72, 142, 146, 144 and 143 °C, respectively. On the other hand, the complex **5** dehydrate in two steps with evolution of 1 mol of H_2O at 74 °C and the other one at 139 °C with mass loss of 4.17 and 4.23/4.66%. These data show that the complex dehydrate in two well-separated steps due to the presence of a loosely bound lattice water molecule ($\Delta H = +88$ J g^{-1}) and more strongly bound one ($\Delta H = +259$ J g^{-1}). The complexes **2–6** have melting points at 193, 190, 180, 189 and 198 °C as shown by their endothermic DTA changes.

Table 7 DTA of the vanadyl complexes of the metformin Schiff-bases

Complex number	Temp. range/°C	DTA temp./°C	ΔH/J g^{-1}	Process
HL^1 [24]	160–213	195 endo.	+89	Melting
	238–284	255 endo.	–	Partial decomposition
	313–365	343 exo.	–190	Partial decomposition
	500–530	530 exo.	–210	Final decomposition
1	58–125	72 endo.	+441	Dehydration
	125–200	155 endo.	+194	Partial decomposition
	312–420	347 endo.	+116	Coordinated water
		407 exo.		Ligand decomposition
	420–522	479 exo.	–508	Final decomposition
2	107–173	142 endo.	+451	Dehydration
	180–234	193 endo.	–	Melting
		224 endo.		Partial decomposition
	272–343	308 endo.	+170	Coordinated water
	343–371	356 endo.	–	Ligand decomposition
	428–482	465 exo.	−103	Final decomposition
	482–565	529 exo.	−381	Reduction
3	114–175	146 endo.	+373	Dehydration
	175–203	190 endo.	–	Melting
	203–232	218 exo.	−174	Partial decomposition
	260–348	309 endo.	+323	Coordinated water
	348–375	358 endo.	–	Ligand decomposition
	496–543	525 exo.	−142	Reduction
4	123–168	144 endo.	+370	Dehydration
	168–193	180 exo.	–	Melting
	193–236	236 endo.	–	Partial decomposition
	288–344	314 endo.	+199	Coordinated water
	344–372	357 endo.	–	Ligand decomposition
	449–551	506 exo.	−446	Reduction
5	41–115	74 endo.	+88	Dehydration
	115–174	139 endo.	+259	Dehydration
	174–207	189 endo.	–	Melting
	252–300	237 endo.	+107	Partial decomposition+
				Coordinated water
	300–374	336 endo.	–	Coordinated water
	415–589	473 exo.	−2540	Ligand decomposition
		536 exo.		Reduction
6	111–163	143 endo	+535	Dehydration
	163–225	198 endo.	+75	Melting
	225–254	230 endo.	–	Partial decomposition
	255–337	279 endo.	+237	Coordinated water +
				Ligand decomposition
	356–389	376 endo.	+105	Final decomposition
	426–567	480 exo.	−1750	Reduction
		510 exo.		

Comparing with TG of HL^1 [24], the second decomposition stage concerns with evolution of $NH(CH_3)_2$ species for the complexes **1–4** and **6**. It has DTG peaks at 152, 218, 219, 216 and 205 °C which bring weight loss of (found/calc.): 12.45/13.11%, 12.89/12.22%, 12.83/12.22%, 12.1/12.22% and 11.19/11.16%, respectively. Endothermic

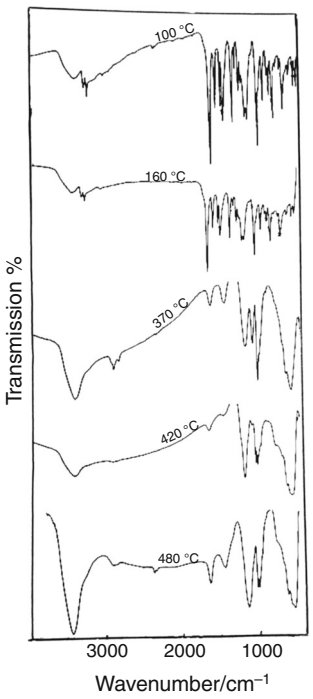

Fig. 3 IR spectrum of the complex (**1**) at different temperatures

DTA peaks taking place at 155, 224, 218, 236 and 230 °C, respectively, confirm this decomposition. It is noticed that this step takes place at the lowest temperature for the complexes **1** and **6**. This may be due to the stronger interaction between V ion and –C=N group of the metformin species of the Schiff-base through covalent bond formation which leads to weakening of the C–N bond of the group C–N$(CH_3)_2$ resulting in its rupture at low temperature. The third stage is a broad one in the 201–378, 273–343, 259–348, 257–344 and 243–333 °C range with DTG maxima at 364, 302, 303 and 307, 278 °C, respectively, which represents decomposition of coordinated water for the above-mentioned complexes which is confirmed by endothermic DTA peaks at 347, 308, 309, 314 and 279 °C, respectively. This shows that the coordinated water in the complex **1** evaporates at the higher temperature in the above series of the complexes. It reflects the strong bonding in the coordination sphere of the complex **1** due to the formation of covalent bond where deprotonation of the metformin C=NH group takes place.

The second and third decomposition steps for the complex **5** include vaporization of H_2O + $NH(CH_3)_2$ and H_2O + $NH(CH{=}NH)_2$ at 225 and 318 °C accompanied with endothermic DTA peaks at 237 and 336 °C. This decomposition mode reinforces the presence of two coordinated water molecules in two different positions in the complex structure. Final decomposition of this complex is obtained at 477 °C with loss of the species C_6H_6 + H_2O + NH=CH associated with endothermic DTA peak at 473 °C. The complex **1** shows the final decomposition step at 467 °C (exothermic DTA = 479 °C) with the formation of VO as a final residue. Note that the molar masses of the removed and remaining species in every step for the complexes **3** and **5** were found to match with mass spectral fragments of the same value (Table 4), which indicates the reliability of the decomposition scheme proposed.

The complexes **2–6** have V metal as a final product. This may be due to reduction of the VO—formed as a final product—to V which takes place at 527, 523, 507, 539 and 516 °C with loss of ½ − ¾ O_2 associated with exothermic DTA maxima at 529, 525, 506, 536 and 510 °C, respectively. The reduction is completed due to the presence of carbonaceous material resulting from the ligand decomposition [44].

Generally, the final decomposition of the Schiff-base in the complexes **2–4** (0.8L) takes place in one step at 352 and 356 °C, which may reflect similarity in the coordination sphere. On the other hand, final decomposition in the complexes **1** and **6** takes place at higher temperature and in two steps at 415,467 and 375,441 °C, respectively. This probably indicates a different bonding in coordination sphere compared to the other series of complexes as shown above.

Mechanism of thermal decomposition

The IR spectrum of the complex **1** heated at 100, 160, 370, 420 and 480 °C is shown in Fig. 3. It shows that the IR spectrum changes shape, intensity and position of some characteristic bands. Heating the complex at 100 °C, its IR spectrum shows the disappearance of the broad band at 3414 cm^{-1} indicating dehydration [30]. Also, medium broad band shown at 3432 cm^{-1} may be due to coordinated water. The υ(NH) bands are shifted to 3317 and 3263; besides, υ(C=N) appears as a sharp band at 1616 cm^{-1}. Heating the complex at 160 °C, distinct bands of υ(CH_3) at 3084 and 2977 cm^{-1} were not observed, indicating cleavage of the ligand and evolution of $NH(CH_3)_2$ species. IR spectrum of heated sample at 370 °C showing new medium broad band at 3440, 2923, 2854 and 1622 cm^{-1} may be assigned to υ(OH), υ(CH_2) and δ(OH). Also, υ(NH) frequency completely disappeared, referring to cleavage of the metformin part in the Schiff-base. Appearance of new bands at 3480 and 1626 cm^{-1} in the IR spectrum of heated sample at 420 °C refers to the formation of a mixture of aqua-hydroxo species [45]. IR bands characteristic for the presence of vanadium oxide is shown as strong broad band at 533 cm^{-1} and medium split band at 1009 and 988 cm^{-1} [46]. Proposed mechanism of thermal decomposition of the complex **1** is shown as follows:

Table 8 Effect of metformin (20 and 40 mg/kg) and the complexes **1** and **4** on survival %, blood glucose, total cholesterol and serum ALT and AST activities in the experimental groups

Groups	Survival %	Blood glucose/mg dL^{-1}	Total cholesterol/mg dL^{-1}	ALT/U L^{-1}	AST/U/L^{-1}
Vehicle	100	79.99 ± 6.66	69 ± 10.4	24.5 ± 4	76.8 ± 3
Diabetic	83.33	401.67 ± 35.87	126 ± 11*	44.5 ± 5*	65.9 ± 7
Metformin (20 mg/kg)	100	212.3 ± 34.95*	129 ± 13*	56.5 ± 5*	126.4 ± 20*^{D}
Metformin (40 mg/kg)	100	188.5 ± 1.8*	121 ± 29*	52.3 ± 5*	128 ± 20*^{D}
Complex **1** (20 mg/kg)	83.33	163.4 ± 17.9*	126 ± 31*^{M}	56.5 ± 6*	88.18 ± 14^{DM}
Complex **1** (40 mg/kg)	83.33	144.25 ± 47.67*	100 ± 41*^{M}	51.7 ± 5*	97.39 ± 21*^{DM}
Complex **4** (20 mg/kg)	100	165.5 ± 13.64*	72 ± 17^{DM}	49.3 ± 5*	85.81 ± 4^{DM}
Complex **4** (40 mg/kg)	100	101.2 ± 8.08*^{M}	55 ± 6^{DM}	47 ± 5*	101.5 ± 6*^{DM}

Results are expressed as mean ± SEM and analyzed using one-way ANOVA followed by Bonferroni's post hoc test

ALT alanine aminotransferase, *AST* aspartate aminotransferase

* $P < 0.05$ compared to vehicle group

^{D} $P < 0.05$ compared to diabetic group

^{M} $P < 0.05$ compared to corresponding metformin group

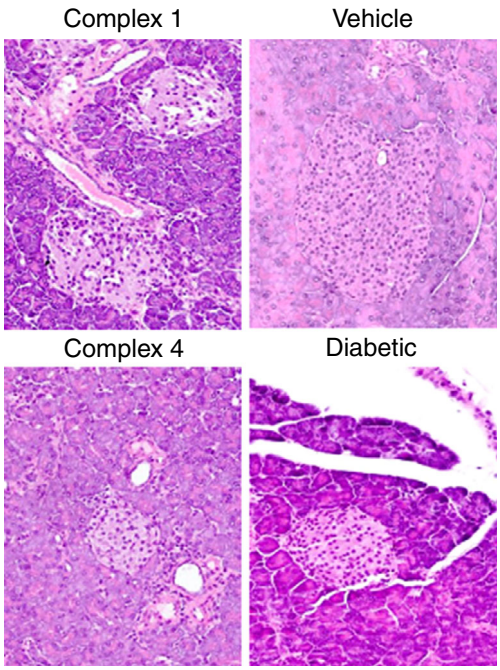

Fig. 4 Sections from the pancreas stained with hematoxylin and eosin

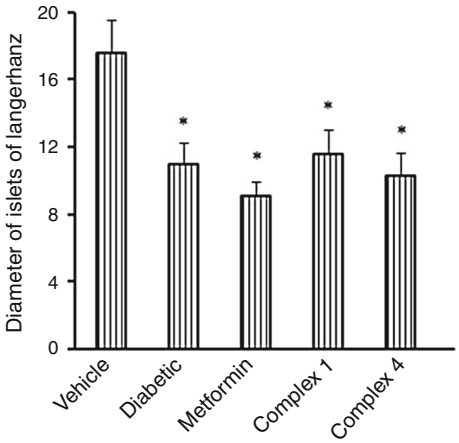

Fig. 5 Mean diameter for pancreatic islets in the experimental groups

Insulin-enhancing studies

In the current study, injection of mice using alloxan (150 mg kg^{-1}) produced hyperglycemia that was confirmed one week after injection and those with fasting blood glucose greater than 200 mg/dL were considered diabetic. The cytotoxic effects of alloxan are due to its active damaging insulin-secreting β-pancreatic cells, leading to increased blood sugar level [47]. At the end of the therapeutic period (14 days), mice treated with metformin showed blood glucose levels lower than that measured in diabetic control group ($P < 0.05$, Table 8) by 47.14 (20 mg kg^{-1}) and 53.07% (40 mg kg^{-1}). Similarly, mice treated with the complexes **1** and **4** showed also lower blood glucose values of 59.31, 58.79 (20 mg kg^{-1}) and 64.98, 74.8% (40 mg kg^{-1}). These results suggested that these complexes have a potential blood glucose-lowering effect equivalent to previous complexes [8–12]. The diabetic control mice showed 83.33% survival, while mice treated with vanadium complexes showed 83.33–100% survival, indicating appropriate degree of safety.

Measuring serum total cholesterol highlighted that treatment with metformin did not significantly modify the total cholesterol level compared to diabetic control. Mice treated with the complex **1** (40 mg kg^{-1}) showed lower serum cholesterol compared to mice treated with metformin. On the

other hand, mice treated with the complex **4** (20 or 40 mg kg^{-1}) showed lower serum total cholesterol compared to diabetic control as well as metformin group.

AST and ALT liver enzymes are released to circulation when liver cells are damaged by alloxan including muscle injury and viral hepatitis as well as cardiac problems. Estimation of liver enzyme activities indicated that ALT activity was greater in diabetic mice compared to vehicle control. Regarding AST activity, all the tested complexes as well as metformin produced significant increase in serum AST activity in comparison with diabetic control group ($P < 0.05$, Table 8). Increased levels of AST and ALT are indicative of cellular damage and make disorder in the functional activity of lever cell membrane. Cases were recorded in which elevation in serum ALT and AST represented pseudohepatotoxicity associated with metformin therapy [48–51].

Photographs for sections from the pancreas stained with hematoxylin and eosin show that diabetic control group have smaller diameter for Langerhans islets compared to vehicle control (Fig. 4). None of the implemented agents produced a significant change in the islet diameter compared to diabetic control (Fig. 5). We can conclude from the results that the new compounds, similar to metformin, control hyperglycemia by extrapancreatic mechanisms. They did not improve the integrity of islets of Langerhans.

Supplementary materials

This attached file contains NMR and GC-mass spectra of the Schiff-base and the UV–Vis spectra of complexes **1** and **6** (as an example).

Conclusions

Because of the global increase in type II diabetes mellitus, there is a need to develop new antidiabetic agents. We have synthesized vanadyl complexes of Schiff-bases of metformin with each of salicylaldehyde (HL^1); 2,3-dihydroxybenzaldehyde (H_2L^2); 2,4-dihydroxybenzaldehyde (H_2L^3); 2,5-dihydroxybenzaldehyde (H_2L^4); 3,4-dihydroxybenzaldehyde (H_2L^5); and 2-hydroxynaphthaldehyde (HL^6) by template reaction. The new compounds are characterized through elemental analysis, conductivity measurements, magnetic moment, IR, UV–Vis, ESR and mass spectroscopy. The complexes have square pyramidal structure with μ values of pentacoordinated vanadyl ion. TG, DTG and DTA confirm the proposed stereochemistry. Mechanism of thermal decomposition of the complex **1** was shown by recording its IR spectra at different temperatures. The complexes **1** and **4** have a potential blood glucose-lowering effect equivalent to previously studied vanadyl complexes.

References

1. Noblía P, Baran EJ, Otero L, Draper P, Cerecetto H, González M, Piro OE, Castellano EE, Inohara T, Adachi Y, Sakurai H, Gambino D. New vanadium(V) complexes with salicylaldehyde semicarbazone derivatives: synthesis, characterization, and in vitro insulin-mimetic activity-crystal structure of[VvO2(salicylaldehyde semicarbazone)]. Eur J Inorg Chem. 2004;2004:322–8.
2. Delgado TC, Tomaz AI, Correia I, Jones JG, Geraldes GFGC, Castro MMCA. Uptake and metabolic effects of insulin mimetic oxovanadium compounds in human erythrocytes. J Inorg Biochem. 2005;99:2328–39.
3. Sakurai H, Sano H, Takino T, Yasui H. An orally active antidiabetic vanadyl complex, bis(1-oxy-2-pyridinethiolato)oxovanadium(IV), with $VO(S_2O_2)$ coordination mode; in vitro and in vivo evaluations in rats. J Inorg Biochem. 2000;80:99–105.
4. Sakurai H, Tsuji A. In: Nriagu JO, editor. Vanadium in the environment, Par 2: health effects. New York: Wiley; 1998. p. 297.
5. Sakurai H, Fujii K, Fujimoto S, FujisawaY, Takechi K, Yasui H, in Tracy AS, Chans DC editors. Vanadium compounds: chemistry, biochemistry, and therapeutic applications, ACS Symposium Series 711, American Chemical Society, Washington, DC, 1998, p. 344.
6. Sakurai H, Fujisawa Y, Fujimoto S, Yasaui H, Takino T. Role of vanadium in treating diabetes. J Trace Elem Exp Med. 1999;12:393–401.
7. Durai N, Saminathan G. Insulin-like effects of bis-salicylidine ethylenediiminato oxovanadium(IV) complex on carbohydrate-metabolism. J Clin Biochem Nutr. 1997;22:31–9.
8. Xie M, Xu G, Li L, Liu W, Niu Y, Yan S. In vivo insulin-mimetic activity of [N, N'-1,3-propyl-bis(salicyladimine)]oxovanadium(IV). Eur J Med Chem. 2007;42:817–22.
9. Bastos AMB, da Silva JG, Maia PIS, Deflon VM, Batista AA, Ferreira AVM, Botion LM, Niquet E, Beraldo H. Oxovanadium(IV) and (V) complexes of acetylpyridine-derived semicarbazones exhibit insulin-like activity. Polyhedron. 2008;27:1787–94.
10. Mendes IC, Botion LM, Ferreira AVM, Castellano EE, Berlado H. Vanadium complexes with 2-pyridineformamide thiosemicarbazones: in vitro studies of insulin-like activity. Inorg Chim Acta. 2009;362:414–20.
11. Nejo AA, Kolawole GA, Opoku AR, Wolowska J, OBrien P. Synthesis, characterization and preliminary insulin-enhancing studies of symmetrical tetradentate Schiff base complexes of oxovanadium(IV). Inorg Chim Acta. 2009;362:3993–4001.
12. Moroki T, Yasui H, Adachi Y, Yoshizawa K, Tsubura A, Ozutsumi K, Katayama M, Yoshikawa Y. New insulin-mimetic and hypoglycemic hetero-binuclear Zinc(II)/oxovanadium(IV) complex. Curr Inorg Chem. 2014;4:54–8.
13. Stepensky D, Friedman M, Srour W, Raz I, Hoffman A. Preclinical evaluation of pharmacokinetic–pharmacodynamic rationale for oral CR metformin formulation. J Control Release. 2001;71:107–15.
14. Babykutty PV, Parbhakaran CP, Anantaraman R, Nair CGR. Electronic and infrared spectra of biguanide complexes of the 3d-transition metals. J Inorg Nucl Chem. 1974;36:3685–8.
15. Subasinghe S, Greenbaum AL, McLean P. The insulin-mimetic action of Mn^{2+}: involvement of cyclic nucleotides and insulin in the regulation of hepatic hexokinase and glucokinase. Biochem Med. 1985;34:83–92.
16. Zhu M, Lu L, Yang P, Jin X. Bis(1,1-di-methyl-biguanido)copper(II) octahydrate. Acta Crystallogr. 2002;E58:m217–9.
17. Patrinoiu G, Patron L, Carp O, Stanica N. Thermal behaviour of some iron(III) complexes with active therapeutically biguanides. J Threm Anal Calorim. 2003;72:489–95.

18. Olar R, Badea M, Cristurean E, Lazar V, Cernat R, Balotescu C. Thermal behavior, spectroscopic and biological characterization of Co(II), Zn(II), Pd(II) and Pt(II) complexes with *N,N*-dimethylbiguanide. J Therm Anal Calorim. 2003;80:451–5.
19. Al-Saif FA, Refat MS. Synthesis, spectroscopic, and thermal investigation of transition and non-transition complexes of metformin as potential insulin-mimetic agents. J Therm Anal Calorim. 2013;111:2079–96.
20. Woo LCY, Yuen VG, Thompson KH, McNeill JH, Orvig C. Vanadyl–biguanide complexes as potential synergistic insulin mimics. J Inorg Biochem. 1999;76:251–7.
21. Gao J. A weak hydrolytical copper(II) complex derived from condensation of *N,N*-dimethylbiguanide with 2-pyridinecarbaldehyde synthesis, crystal structure and biological activity. Synth React Inorg Met-Org Chem Nano-Met Chem. 2007;37:621–5.
22. Olar R, Badea M, Marinescu D, Iorgulescu E, Stoleriu S. Ni(II) complexes with ligands resulted in condensation of *N,N*-dimethylbiguanide and pentane-2,4-dione. J Therm Anal Calorim. 2005;80:363–7.
23. Treviño S, Sánshez-Lara E, Sarmiento-Ortega VE, Sánshez-Lombardo I, Flores-Hernádez JÁ, Pérez-Benítez A, Barmbila-Colombres E, González-Vergara E. Hypoglycemic, lipid-lowering and metabolic regulation activities of metforminium decavnadate $(H_2Metf)_3[V_{10}O_{28}].8H_2O$ using hypercaloric-induced carbohydrate and lipid deregulation in Wistar rates as biological model. J Inorg Biochem. 2015;147:85–92.
24. Mahmoud MA, Zaitone SA, Ammar AM, Sallam SA. Synthesis, structure and antidiabetic activity of chromium(III) complexes of metformin Schiff-bases. J Mol Struct. 2016;1108:60–70.
25. Figgis BN, Lewis J. Magnetochemistry of complex compounds in modern coordination chemistry. In: Lewis J, Wilkins RG editor. New York: Wiley; 1960.
26. Federiuk IF, Casey HM, Quinn MJ, Wood MD, Ward WK. Induction of type-1 diabetes mellitus in laboratory rats by use of alloxan: route of administration, pitfalls, and insulin treatment. Comp Med. 2004;54:252–7.
27. Geary WJ. The use of conductivity measurements in organic solvents for the characterisation of coordination compounds. Coord Chem Rev. 1971;7:81–122.
28. Nakamoto K. Infrared and Raman spectra of inorganic and coordination compounds. Part II: applications in coordination, organometallic, and bioinorganic chemistry. 5th ed. New York: Wiley; 1997.
29. Abd-Elzaher MM. Spectroscopic characterization of some tetradentate Schiff bases and their complexes with nickel, copper and zinc. J Chin Chem Soc. 2001;48:153–8.
30. Boas LV, Bessoa JC. Vanadium, comprehensive coordination chemistry, vol. 3. In: Wilkinson G, Gillard RD, McCleverty JA editors. New York: Pergamon; 1978. p. 455.
31. Kolawole GA, Patel KS. The stereochemistry of oxovanadium(IV) complexes derived from salicylaldehyde and polymethylenediamines. J Chem Soc Dalton Trans. doi:10.1039/DT9810001241.
32. Patel KS, Kolawole GA, Earnshaw A. Spectroscopic and magnetic properties of Schiff base complexes of oxovanadium(IV) derived from 3-methoxysalicylaldehyde and aliphatic diamines. J Inorg Nucl Chem. 1981;43:3107–12.
33. Pearson RG. Hard and soft acids and bases. J Am Chem Soc. 1963;85:3533–9.
34. Lever ABP. Electronic spectra of some transition metal complexes: derivation of Dq and B. J Chem Edu. 1968;45:711–2.
35. Ballhausen CJ, Gray HB. the electronic structure of the vanadyl ion. Inorg Chem. 1962;1:111–22.
36. Reynolds JG, Sendlinger SC, Murray AM, Huffman JC, Christou G. Synthesis and characterization of vanadium(II, III, IV) complexes of pyridine-2-thiolate. Inorg Chem. 1995;34:5745–52.
37. Nejo AA, Kolawole GA, Opoku AR, Muller C, Wolowska J. Synthesis, characterization, and insulin-enhancing studies of unsymmetrical tetradentate Schiff-base complexes of oxovanadium(IV). J Coord Chem. 2009;62:3411–24.
38. Kolawole GA, Patel KS. Spectroscopic and magneto-chemical investigation oxovanadium(IV) 5-chlorosalicylaldiimines. J Coord Chem. 1982;12:121–7.
39. Cornman CR, Geiser-Bush KM, Rowley SP, Boyle PD. Structural and electron paramagnetic resonance studies of the square pyramidal to trigonal bipyramidal distortion of vanadyl complexes containing sterically crowded schiff base ligands. Inorg Chem. 1997;36:6401–8.
40. Sasmal PK, Saha S, Majumdar R, De S, Dighe RR, Chakravarty AR. Oxovanadium(IV) complexes of phenanthroline bases: the dipyridophenazine complex as a near-IR photocytotoxic agent. Dalton Trans. 2010;39:2147–58.
41. Yadava AK, Yadav HS, Saxena R, Rao DP. Syntheses and spectral studies of oxovanadium(IV) Schiff base complexes derived from 1,1′-oxalyldiimidazole and aromatic amines. Eur Chem Bull. 2015;4:356–9.
42. Lu L-P, Yang P, Qin S-D, Zhu M-L. Bis[1,1-di-methyl- biguanide(1–)-κ2N2, N5]copper(II) monohydrate. Acta Cryst. 2004;C60:m219–20.
43. Olar R, Dogaru A, Marinescu D, Badea M. New vanadyl complexes with metformin derivatives as potential insulin mimetic agents. J Therm Anal Calorim. 2012;110:257–62.
44. Bauer G, Güther V, Hess V, Otto A, Roidl O, Roller H, Sattelberger S. Vanadium and vanadium compounds, Ullmann's encyclopedia of industrial chemistry. London: Wiley; 2000.
45. Carp O, Gingasu D, Mindru I, Patron L. Thermal decomposition of some copper–iron polynuclear coordination compounds containing glycine as ligand, precursors of copper ferrite. Thermochim Acta. 2006;449:55–60.
46. Nyquist RA, Kagel RO. Infrared spectra of inorganic compounds. New York: Academic Press; 1971.
47. Arslan H, Özpozn N, Tarkan N. Kinetic analysis of thermogravimetric data of p-toluidino-p-chlorophenylglyoxime and of some complexes. Thermochim Acta. 2002;383:69–77.
48. Lenzen S. The mechanisms of alloxan- and streptozotocin-induced diabetes. Diabetlogia. 2008;51:216–26.
49. Swislocki AL, Noth R. Case report: pseudohepatotoxicity of metformin. Diab Care. 1998;21:677–8.
50. Cone CJ, Bachyrycz AM, Murata GH. Hepatotoxicity associated with metformin therapy in treatment of type 2 diabetes mellitus with nonalcoholic fatty liver disease. Ann Pharmacother. 2010;44:1655–9.
51. Saadi T, Waterman M, Yassin H, Baruch Y. Metformin-induced mixed hepatocellular and cholestatic hepatic injury: case report and literature review. Int J Gen Med. 2013;6:703–6.